Design and Test of Spatial Cognitive Training and Evaluation System Based on Virtual Reality Head-Mounted Display With EEG Recording

Dong Wen, *Member, IEEE*, Jingpeng Yuan, Jingjing Li, Yue Sun, Xianpu Wang, Ruihang Shi, Xianglong Wan, *Member, IEEE*, Yanhong Zhou, Haiqing Song, Xianling Dong, Fangzhou Xu, Xifa Lan, and Tzyy-Ping Jung

***Abstract*— The field of spatial cognitive training and evaluation has rapidly evolved. However, the low learning motivation and engagement of the subjects hinder the widespread use of spatial cognitive training. This study designed a home-based spatial cognitive training and evaluation system (SCTES), which aimed to train subjects on spatial cognitive tasks for 20 days, and compared the brain activities before and after the training. This study also evaluated the feasibility of using a portable all-in-one prototype for cognitive training that combined a virtual reality (VR) head-mounted display with high-quality electroencephalogram (EEG) recording. During the course of training, the length of the navigation path and the distance between the starting position and the platform position revealed significant behavioral differences. In the testing sessions, the subjects showed significant behavioral differences in the time it took to complete the test task before and after training. After only four days of training, the subjects demonstrated significant differences in the Granger causality analysis (GCA) characteristics of brain regions in the δ, θ, α_1, β_2, and γ frequency bands of the EEG, as well as significant differences in the GCA of the EEG in the β_1, β_2, and γ frequency bands between the two test sessions. The proposed SCTES used a compact and all-in-one form factor to train and evaluate spatial cognition and collect EEG signals and behavioral data simultaneously. The recorded EEG data can be used to quantitatively assess the efficacy of spatial training in patients with spatial cognitive impairments.**

***Index Terms*— EEG, spatial cognition training and evaluation system, virtual reality head-mounted display.**

Manuscript received 7 August 2022; revised 16 January 2023 and 2 May 2023; accepted 27 May 2023. Date of publication 6 June 2023; date of current version 20 June 2023. This work was supported in part by the National Natural Science Foundation of China under Grant 62276022, Grant 62206014, Grant 61876165, and Grant 61503326; and in part by the National Key Research and Development Program of China under Grant 2021YFF1200603. *(Corresponding authors: Yanhong Zhou; Fangzhou Xu; Tzyy-Ping Jung.)*

This work involved human subjects or animals in its research. Approval of all ethical and experimental procedures and protocols was granted by the Ethics Committee of First Hospital of Qinhuangdao in Hebei Province, China, under Application No. 2018B006, in 2018.

Dong Wen and Xianglong Wan are with the Key Laboratory of Perception and Control of Intelligent Bionic Unmanned Systems, Ministry of Education, School of Intelligence Science and Technology, University of Science and Technology Beijing, Beijing 100083, China.

Jingpeng Yuan, Jingjing Li, Yue Sun, Xianpu Wang, and Ruihang Shi are with the Key Laboratory for Computer Virtual Technology and System Integration of Hebei Province, School of Information Science and Engineering, Yanshan University, Qinhuangdao, Hebei 066004, China.

Yanhong Zhou is with the School of Mathematics and Information Science and Technology, Hebei Normal University of Science and Technology, Qinhuangdao, Hebei 066004, China (e-mail: yhzhou168@163.com).

Haiqing Song is with the Department of Neurology, Xuanwu Hospital of Capital Medical University, Beijing 100053, China.

Xianling Dong is with the Hebei Key Laboratory of Nerve Injury and Repair, Chengde Medical University, Chengde, Hebei 067000, China.

Fangzhou Xu is with the School of Optoelectronic Engineering International, Qilu University of Technology (Shandong Academy of Sciences), Jinan, Shandong 250353, China (e-mail: xfz@qlu.edu.cn).

Xifa Lan is with the Department of Neurology, First Hospital of Qinhuangdao, Qinhuangdao, Hebei 066000, China.

Tzyy-Ping Jung is with the Swartz Center for Computational Neuroscience, University of California, San Diego, San Diego, CA 92093 USA (e-mail: jungtp2013@gmail.com).

Digital Object Identifier 10.1109/TNSRE.2023.3283328

I. Introduction

SPATIAL cognition is a high-order cognitive function that includes spatial observation, spatial memory, spatial imagination, spatial thinking, and other abilities. It is responsible for recording information related to the environment, spatial direction, and spatial relationships, which is reflected in working memory, both short-term and long-term memory [1], [2]. Spatial cognitive training and evaluation is a rapidly growing field in cognitive science [3], [4], [5] and is also of great significance in the diagnosis and rehabilitation of mild cognitive impairment (MCI) patients who often have problems with spatial orientation [6], [7]. An effective spatial cognition training requires subjects' full engagement and the training content should be closely related to the subjects' daily lives [8], [9].

Virtual reality (VR) [9] and brain-computer interfaces (BCIs) [10] are emerging technologies in spatial cognitive training and evaluation [11], [12]. VR meets the subjects' social requirements, and may be used as the primary method for spatial cognitive training (SCT) [8], [9], [11], [12], [13], [14]. However, the previous studies did not assess the efficacy of the training in near-real-time, making it difficult to adjust or optimize the training accordingly. BCIs based on electroencephalogram (EEG) signals have been used for spatial cognitive training and evaluation in near real-time [15],

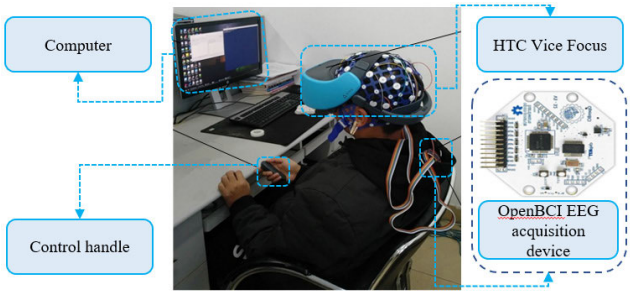

Fig. 1. EEG-HMD system instance diagram.

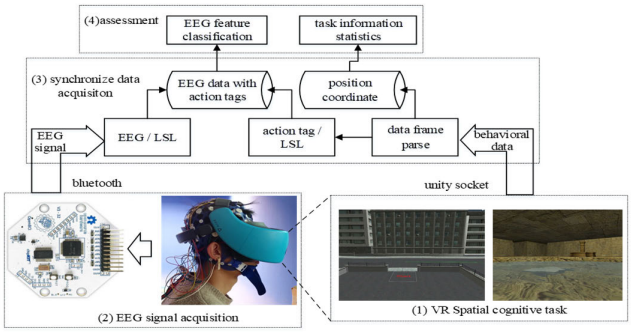

Fig. 2. The architecture diagram of the EEG-HMD -VR system.

[16], [17], [18]. Therefore, it is natural to combine BCIs and VR [19], [20], [21], [22], [23], [24] for spatial cognitive training and evaluation. The preliminary studies [25], [26], [27], [28] showed that BCI-VR is a promising tool for spatial cognitive training and evaluation. However, this tool is still in its infancy, and the technical merit of BCI-VR has not been fully evaluated in these studies. Furthermore, the performance of spatial cognitive training and evaluation needs to be improved. Therefore, to promote the healthy development of the spatial cognitive training and evaluation research field, it is necessary and important to find an effective way to standardize the application of BCI and VR.

Following the basic design principle of the cognitive training system [29], [30], [31], [32], [33] and the research in the Morris water maze task [3], [34], this study used EEG-HMD (head-mounted display) -VR to develop a spatial cognitive training and evaluation system. To be more specific, the system implements the VR water maze task to train the user's spatial cognition and a virtual city roaming task to assess the training's efficacy (i.e., pre-training and post-training tests). This study aims to validate the effectiveness of using a portable EEG device and HMD to collect high-quality EEG during VR-based cognitive training and quantitatively monitor the changes in neural plasticity during the cognitive training, which could assess the training's efficacy and optimize individualized spatial cognitive training. This work's contribution may be summed up as follows:

(1) An EEG-HMD is used to build a system for training and assessing spatial cognition.

(2) It has been demonstrated that a portable integrated HMD can collect high-quality EEG during cognitive training in virtual reality, allowing for the objective and quantitative monitoring of changes in neuroplasticity.

II. Materials and Methods

A. System Platform and Architecture Design

The proposed spatial cognitive training and evaluation system is composed of both software and hardware. The hardware comprises an OpenBCI EEG device, HTC Vive Focus head-mounted display (HMD), a control handle, and a desktop computer, as shown in Fig. 1. The OpenBCI device is used to collect the EEG signals during the experiment. The sampling rate of the device is 125Hz. The wireless OpenBCI module was used to collect 16 channels of EEG data using wet electrodes with an impedance below 10k. The virtual task scene was presented using the HTC Vive Focus HMD. The device is portable and runs on Android 6.0, with a display resolution of 2880∗1600 and a refresh rate of 75Hz. A Vive Focus control handle was used to interact with the VR scene during the experiment.

The software of the system is developed using the Unity 3D game engine, MATLAB programming software platform, and PyCharm development environment. The Unity 3D game engine is used to create 3D virtual task scenarios. The MATLAB software platform is used to analyze the collected EEG signals, and the PyCharm development environment receives synchronized EEG and behavioral data.

Fig. 2 shows the system architecture. The EEG device sends the EEG signals to the computer via Bluetooth. The VR HMD sends the subjects' behavioral data during the task to the computer through the transmission control protocol/Internet protocol (TCP/IP) protocol. The computer receives EEG signals and behavioral data synchronously. Specifically, the computer uses the Lab Streaming Layer (LSL) protocol to broadcast the EEG signals received from the serial port buffer to the local area network. The TCP client parses the behavioral data, forwards the parsed action tags to the local area network through the LSL protocol, and adds the time-stamps to the position coordinate data. Then, the LSL protocol client synchronously receives and aligns the EEG signals and action tags. Finally, spatial cognition is quantitatively evaluated from two aspects: EEG characteristics and path information.

B. VR-Based Spatial Cognitive Training Task

1) Task Design: This system imitates the Morris water maze experiment, which is used to study the spatial cognition and spatial learning ability of rats [34] and transfers the experimental environment to a virtual scene. Inspired by Astur et al. [35] and Horecka [36], a virtual Morris Water Maze (VMWM) is constructed to train spatial cognition, which is similar to the rat water maze task [34], [37]. The subjects repeat the training tasks with different contents to improve their spatial cognitive ability. Each subject attends a training session every day for 20 days.

During the VMWM training, subjects donned the VR HMD and used remote cues (prompt routes) to find the targets in the virtual pool setting (the scene seen in the VR device). In particular, the experiment was divided into two modes: a position navigation mode and a space exploration mode. During the position navigation mode, subjects entered the virtual pool from various locations and began looking for the hidden platform, and the time they spent boarding the platform was recorded. The subjects' spatial cognition and learning ability were evaluated according to the time of multiple

Fig. 3. The scenario interface of the VMWM task.

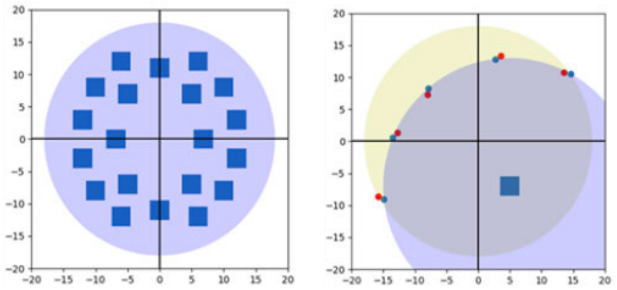

(a) Map of platform location (b) Map of starting position and orientation

Fig. 4. The map of the VMWM task platform and location.

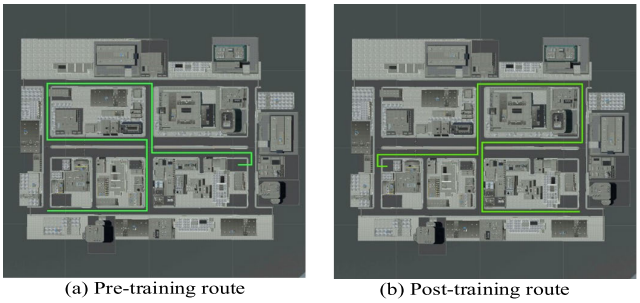

(a) Pre-training route (b) Post-training route

Fig. 5. The map of VCW task road.

experiments. The space exploration experiment mainly tested the subject's memory of where the platform was located. In the experiment, the platform is removed from the pool, and the distance between the subject's selected platform location and the actual platform location was recorded as a measure of their spatial cognitive ability. The training process was divided into three stages, depending on whether the platform was visible:

(1) Visible platform stage. It allows the subjects to learn the task requirements and the platform's location in relation to the remote clues.

(2) Hidden platform stage. It was a repetitive task. To train their spatial cognitive navigation ability, the subjects started from different starting locations and viewing directions, and used the remote clues to find the hidden platform.

(3) Exploratory stage. The platform was removed and the subject used his/her spatial memory to navigate to the platform.

2) Scene Design: The VMWM task consists of two scenes: the menu scene and the task scene. The main functions of the menu scene record (1) basic training information, such as the subject's ID, and the training days; (2) training task selection, such as the entrance of the VMWM with a visible platform, the entrance of the VMWM with an invisible platform, and the entrance of the VMWM during the exploration stage. The task scene (shown in Fig. 3) is set in a square room and uses identical brown bricks on the walls and floors to initially construct a virtual environment without any reference object. Then, a circular pool with a radius of 18 meters was placed in the center of the scene coordinates, and water surface effects of waves and highlights are added to mimic the pool environment used for cognitive experiments. Various objects are scattered around the pool as spatial cues for navigation. Then, a cuboid with the length of 2 meters, the width of 2 meters and the height of 3 meters is placed in the pool as a platform for the Morris water maze experiment. The initial position of the platform is below the water level.

3) Settings of Task Parameters: Because the VMWM task lasts for 20 days, the position of the platform varies daily. Fig. 4(a) shows 20 different locations for all the 20 days. In one day, the positions for the three stages are the same, but the starting positions and direction parameters of the subjects are different. In the visible platform phase, the starting position of the subject is the center of the scene coordinate, the direction parameter is 0, the platform can be triggered to rise, and the task has no time limit. In the hidden platform stage, the position of the platform is at one of the 20 locations, as shown in Fig. 4(a). The starting positions can be one of the five locations centered at the maximum interval on the arc of a circle of radius 20 meters from the platform (the blue point in Fig. 4(b)). But, within each day, some randomness is introduced to the starting points (by placing the subject along the circle of radius 1 meter (centering at each of the blue dots), as shown by the red dots in Fig. 4(b). That is, across all the trials of the hidden platform stage, one of the five candidate points is randomly selected as the starting position of the subject, and the direction candidate point arc corresponding to the point is taken as the starting direction radiance parameter of the subject. The task time was limited to 2 minutes, and the average time for the subjects to accomplish this activity was less than one minute, so it follows that the platform rises on command from the participant. The starting position and direction parameters in the exploration phase are selected in the same way as they are in the hidden platform stage, but the platform cannot be triggered to rise, and the task time is limited to one minute.

C. VR-Based Spatial Cognition Test Task Design

The subject needs to remember the walking route and the surrounding environment. In the testing mode, the green sign of the route is hidden and the subject navigates using the environmental references and his/her cognitive map, which is a mental representation of the spatial layout of an environment.

The VCW task uses a 3D city model with seven symmetrical streets. From a first-person perspective, the subjects use the direction key to control the character object's advancement and left-right rotation. The forward speed is set to 5 m/s, and the rotational angular velocity is set to 10 rad/s. To ensure the consistency of the difficulty levels of the pre-training and the post-training, the two routes are mirror-reversed, that is, the post-training route is the pre-training one rotated by 180 degrees with the middle longitudinal street as the axis. Fig. 5(a) and Fig. 5(b) show the pre-training and post-training routes, respectively.

TABLE I
VR SERVER BEHAVIOR DATA ENCAPSULATION PROTOCOL

data	protocol	examples
role object coordinates	<x>, <z>	14.7,5.3
handle button response code	key<code>	keyL
task execution information	file<id_trial_iteration>	file2_1_1

D. Data Collection

1) EEG Acquisition: The subjects participated in the spatial cognitive task in a quiet room for collecting their EEG data. The subjects first wore the OpenBCI EEG cap of the 16 wet electrodes placed on the scalp at Fp1/Fp2, F7/ F8, F3/F4, Fz, FCz, C3/C4, Cz, P7/P8, Pz, O1/O2 according to the international 10-20 system, referenced to the bilateral earlobes. The data collection was approved by the Ethics Committee of First Hospital of Qinhuangdao in Hebei Province, China (The approval number was 2018B006 in 2018).

2) Collection of Behavioral Data: To analyze the condition of the subjects' task execution and the changes in spatial cognitive ability, we recorded their behavioral data during the experiment. After establishing a connection with the client, the server uses a polling method to detect the movements of the role object in the task scenario, the button responses on the control handle, and the progress of the task, and sends the information to the client. Table I shows the contents of the recorded behavioral data.

When the server detects the movements of the character object, it adds the comma character to the x and z coordinates of the character and sends them to the client as a location data frame. When the direction keys on the controller are detected, key characters are added before the direction code and sent to the client as an active data frame. In the system, the characters F, L, and R correspond to the forward, left turn, and right turn in the task, respectively.

3) Synchronization of the EEG Signals and Behavioral Data: The Python multithreading technology and LSL open-source protocol are used to synchronize the EEG and behavioral data. Specifically, when the computer receives the EEG data frame and behavioral data frame, it aligns the action events and EEG data frame on the time axis, then adds the timestamp of the receiving moment to the position coordinates of the behavioral data and stores it on the computer.

4) EEG Preprocessing: The preprocessing of EEG signals mainly includes filtering, artifact removal, and data segment extraction (Epoching). This study uses the EEGLAB [38] toolbox under the MATLAB environment to perform the preprocessing of EEG signals. Firstly, the EEG signals are band-pass filtered with a 1-45 Hz filter, which retains most of the signals while removing those in unwanted frequency bands (such as 50 Hz power frequency interference). Secondly, the independent component analysis (ICA) is used to remove the electrooculogram and myoelectric artifacts. Thirdly, the EEG signals are divided into the seven frequency bands: δ (1-4 Hz), θ (4-8 Hz), α_1 (8-10.5 Hz), α_2 (10.5-13 Hz), β_1 (13-20 Hz), β_2 (20-30 Hz), and γ (30-40 Hz). Finally, the EEG signals are epoched according to the event markers recorded during the experiment. Considering that the button responses of the subject during the VR task are used as event markers in the system, the time window of the epoch is set to 1 second before and after the button responses. Then, these epoched data are analyzed using the methods described below.

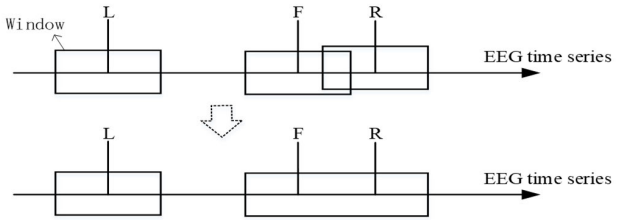

Fig. 6. Schematic diagram of the epoch extraction method for the telescopic time window.

Since the button responses are asynchronous, EEG data within a time window around button presses (event markers) are extracted, as shown in Fig. 6. If two consecutive windows overlapped in time, the two epochs are merged.

In the pre-processing, baseline correction is performed for all extracted epoch data (based on 1 second before the event), and the EEG signals in the frequency bands are combined into a new time series to obtain time series of a total of seven frequency bands. For the EEG signals within each frequency band, the sample is extracted using a moving window, with a window width of two seconds, a step size of one second, and a 50% overlap. After segmenting the EEG signals, we found that the sample sizes of the EEG data of all subjects in the first four days of training decreased monotonically, with 1420, 1272, 1110, and 949, respectively. As the subjects became accustomed to the training, we also found that the sample sizes of the EEG signals decreased from the pre-training to post-training tests. In addition, according to the behavioral data, in the VMWM task training stage, the average path length of all subjects in the hidden platform stage was dramatically reduced from the first day to the fourth day. And the average time spent on tasks decreased significantly from the first day to the fourth day. Therefore, EEG data from the first day to the fourth day were selected for analysis in this paper.

E. Subjects and Task Information

Seven young healthy male subjects participated in this study. They had normal or corrected visual acuity, no color blindness, and no disease history. None of the subjects had participated in an experiment similar to this experiment before, and signed the informed consent form, indicating their willingness to participate in the study. The mean age of the subjects was 24 $\pm$ 1.63 years, ranging from 21 to 26 years old.

All the subjects wore the OpenBCI electrode cap and the HTC Vive Focus virtual head display device and interacted with the VR scene via a control handle. As shown in Fig. 7, the subjects first participated in the pre-training VCW task to assess their spatial cognitive ability, then participated in the VMWM task for 20 days to improve their spatial cognitive ability, and finally performed the post-training VCW evaluation task again. The number of trials per day is 1.

F. Methods of Data Analysis and Statistics

1) Feature Extraction Based on Granger Causality Analysis: This study used the Granger causality analysis (GCA) method

Fig. 7. Experimental procedure.

to examine the causal characteristics and interactions among various brain regions [39], [40], [41]. The underlying concept of GCA is that if past values of time series X and Y are utilized to estimate the current value of time series X, resulting in lower error variance compared to estimates based solely on past values of time series X, then Y is considered the cause of time series X. The Granger causality method involves a multivariate autoregressive model that determines causal relationships by comparing the residual terms of regression variance. The F-test is used to construct the F statistic to determine whether the Granger causality between the variables is statistically significant. The magnitude of the ln(F) value is used to gauge the strength of the causal effect.

2) The Methods of System Evaluation and Statistical Analysis: This study quantitatively assessed the changes in the spatial ability of the subjects before and after training using the recorded behavioral and EEG signals. For the behavioral data, the following five indicators are used to measure subjects' spatial ability.

(1) In the stage of the VMWM hidden platform, the time (in seconds) that subjects spend performing tasks is calculated;

(2) In the stage of the VMWM hidden platform, the path length (in meters) that subjects navigate through the task is calculated;

(3) In the VMWM exploration stage, the distance (in meters) between the platform position selected by the subjects and the actual platform position is calculated.

(4) In the VCW test task, the time spent on the task (in seconds) is calculated.

(5) In the VCW test task, the completion of the task by the subjects is counted.

This study uses the paired sample T-test statistical method to analyze the significant differences in the behavioral data indexes of the VMWM training tasks (the analyzed data are the behavioral data from the first and last day of training) and uses paired sample T-test and chi-square test statistical methods to exam the significant differences in the time and completion of the two VCW test tasks before and after the training.

For EEG signals, The GCA method is used to extract the eigenvalues of brain regions in each frequency band, and these GCA eigenvalues are used to analyze the spatial cognitive changes of subjects. For the VMWM training, an independent sample t-test is used to analyze the change in GCA characteristics during the first four days of training. The GCA characteristics for the first and fourth days are compared in detail. For the VCW testing, we use the independent sample t-test to analyze the differences in the GCA characteristics for each brain region between the pre- and post-training VCW tasks. The specific methods are detailed as follows:

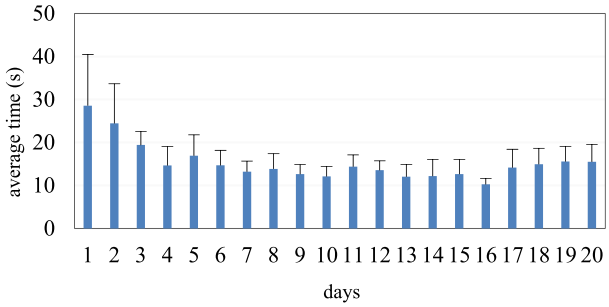

Fig. 8. The average task execution time of the subjects in the VMWM hidden-platform stage in the entire training cycle. The x-coordinate represents the number of days of training (x= 1,2,3 . . . , 20), and the ordinate represents the average time spent by the subjects on the task (in seconds, the blue column represents the average time consumed, and the black line represents the standard deviation).

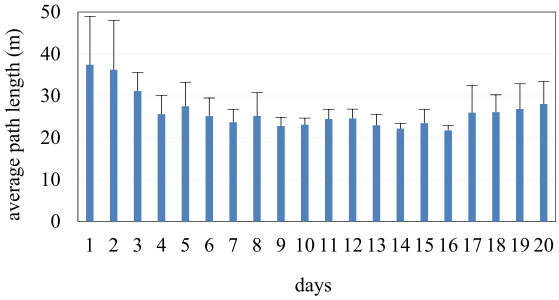

Fig. 9. The average navigation path length of the subjects in the VMWM hidden-platform stage in the whole training cycle: the x-coordinate represents the training days (x= 1,2,3 . . . , 20), and the ordinate represents the average path length of the subject's navigation during the task (in meters, the blue bars represent the average path length, and the black lines represent the standard deviation).

(1) First, the EEG signals of the subjects during the first four days of the VMWM task and the EEG signals tested before and after the VCW task were selected and pre-processed using the method described in Section D.4 to obtain two types of sample data in seven frequency bands.

(2) EEG features are extracted using the method described above for each frequency band and channel combination.

(3) Independent sample T-test method is used to analyze the significant differences in EEG signal characteristics in each frequency band and channel combination. After the corresponding p-value is obtained through the T-test, a false discovery rate (FDR) check is performed on the p-value. The p-value was used to judge whether there were significant differences in the GCA characteristics of each brain region combination after four days of VMWM training and between the two VCW test tasks.

III. Results

A. Behavioral Data Analysis Results

1) Behavioral Data During Training: Fig. 8 shows the average time spent in the hidden-platform phase of the VMWM task throughout the training. The overall time spent on the task decreased across days. The paired-sample T-test showed that the time taken to complete the hidden platform task on the first day (28.54 ± 11.91) was significantly longer than that on the last day (15.49 ± 4.09), $p < 0.05$.

Fig. 9 shows the average navigation path length for all the subjects in the hidden-platform phase throughout the training phase of the VMWM task. In general, the overall path length

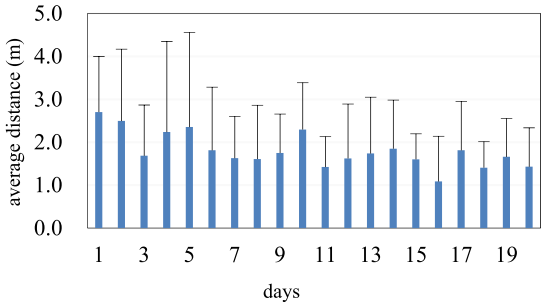

Fig. 10. The differences between the selected position and the average distance between the platform position in the VMWM exploration platform stage in the entire training cycle: the x-coordinate represents the training days (x= 1,2,3 . . . , 20). The ordinate represents the mean distance between the selected platform position and the real platform position (in meters, the blue bars represent the mean distance differences, and the black lines represent the standard deviation).

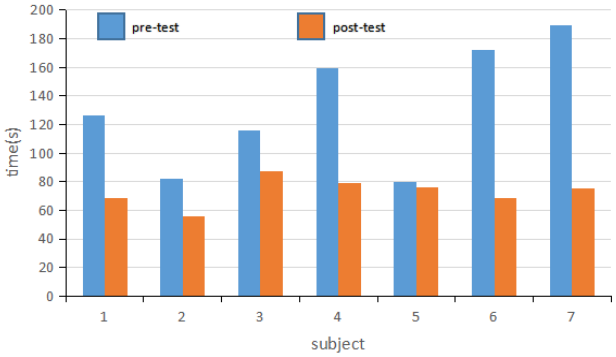

Fig. 11. The time taken by the seven subjects in pre-test (blue bars) and post-test (orange bars) of the VCW task time spent on completing the VCW task is the ordinate, the subject's ID is the abscissa.

decreased across the first four days and then plateaued. The paired sample T-test statistics showed that the path length in the hidden platform task on the first day (37.38±11.54) was significantly longer than that on the last day (28.03±5.38), $p<0.05$.

Fig. 10 shows the average distance between the subjects' selected locations and the actual platform locations during the exploration platform phase of the VMWM task throughout the training sessions. The discrepancy across subjects is generally decreasing over time. The paired sample T-test statistical results showed that the discrepancy on the first day (2.7±1.3) was significantly higher than that on the last day (1.43±0.91), $p<0.05$.

2) Task Performance of the VCW Task Before and After Training: (1) Compare the difference in task completion and path between the two test games

Fig. 11 shows the amount of time spent on the VCW tasks before and after the 20-day training. In the second test, the subjects took significantly less time to complete the task than they did in the first test. The paired sample T-test showed that the differences were statistically significant ($p = 0.00942$).

(2) Compare the difference in task completion and path between the two test games

Fig. 12 shows the path and task completion subject no.2 and no.4 in the VCW task before and after the VMWM training. In the pre-training test, only test subject no.4 completed the task, while the other subjects could not, and the task completion degree was 1/7. In the post-training test, all the

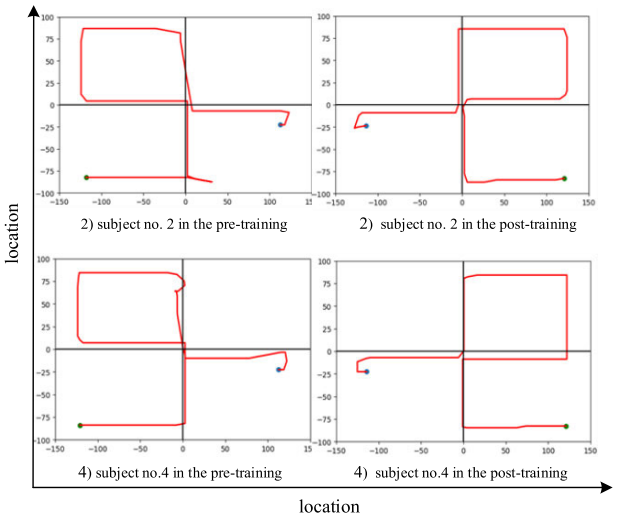

Fig. 12. The path diagram of subject no.2 and no.4 in the pre-training and post-training VCW tasks.

subjects completed the task with a task completion degree of 1. The result of the Chi-square test of the task completion of subjects in the pre-training and post-training tests showed that the p-value is 0.005, showing that the task completion degree of subjects in the pre-training and post-training tests was significantly different.

B. The Differences in Connectivity the First Four Days of Training

This study exams the changes in EEG spectra in the seven frequency bands of the δ, θ, α_1, α_2, β_1, β_2, and γ during the first four days of the training. First, the GCA method is used to extract the eigenvalue ln (F) of the EEG data over the four days, and the mean value of the ln (F) of each brain region combination in each frequency band is calculated as an index of causal strength of each brain region. Finally, the independent sample t-test is used to examine the GCA characteristics of the first and fourth day of training, and the statistical p-value is checked using FDR. Only a combination of brain regions with $p < 0.01$ and increasing causal intensity in four days is presented below.

1) δ Frequency Band: The GCA results of δ frequency band activity on the first and fourth days of training are shown below. GCA feature values of brain area combinations including FP1→F3 (0.13, 0.24, 2.41E-42), FP2→F4 (0.14 0.24, 8.27E-40), F3→Pz (0.17, 0.26, 8.77E-25), Fz→FCz (0.11, 0.27, 8.75E-79), Fz→C3(0.16, 0.27, 1.57E-38), F4→F8 (0.08, 0.24, 8.23E-66), FCz→O2 (0.18, 0.26, 2.56E-28), Cz→O2 (0.14, 0.25, 4.83E-44), O1→O2 (0.14, 0.24, 1.64E-33), P7→FP1 (0.16, 0.24, 1.09E-29), O1→FP1 (0.15, 0.27, 4.50E-40), Pz→FP2 (0.17, 0.27, 2.35E-38), FCz→F7 (0.07, 0.26, 5.98E-85), C4→F7 (0.18, 0.29, 7.90E-36), P7→F7 (0.17, 0.25, 1.88E-25), O1→F7 (0.12, 0.27, 4.66E-52), Fz→F3 (0.14, 0.26, 9.14E-49), O1→Fz (0.21, 0.29, 4.12E-26), O2→Fz (0.21, 0.31, 1.09E-28), F8→F4 (0.12, 0.25, 3.51E-56), FCz→F4 (0.15, 0.28, 1.42E-63), C3→F4 (0.24, 0.35, 4.07E-38), Cz→F4 (0.29, 0.41, 1.36E-38), C4→F4 (0.32, 0.42, 7.06E-24), P7→F4 (0.18, 0.26, 3.94E-32), Pz→F4 (0.25, 0.34, 7.66E-32), P8→F4 (0.20, 0.29, 9.45E-35) increase

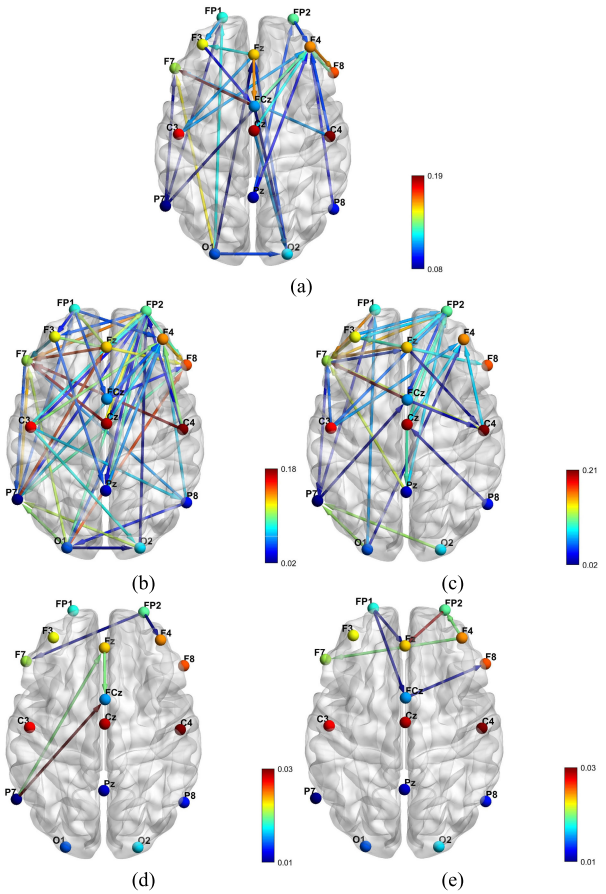

Fig. 13. Visually increased connectivity after four days of training compared to that of the first day training on five frequency bands separately: (a) δ frequency band, (b) θ frequency band, (c) α_1 frequency band, (d) β_2 frequency band, and (e) γ frequency band. The colors represent how much connectivity increased on the fourth day relative to the first day.

gradually from the first to the fourth day, with the fourth day being significantly greater than the first ($p< 0.01$). Note: (0.13, 0.24, 2.41E-42), where '0.13',' 0.24' represents the GCA feature value on the first day and the fourth day respectively, and '2.41E-42' represents the P value of significant difference between GCA feature of the first day and fourth day. Fig. 13(a) showed the increased connectivity visually.

2) θ frequency band: The GCA results of θ frequency band activity on the first and fourth days of training are shown below. GCA feature values of brain area combinations including FP1→F3 (0.15, 0.19, 1.81E-07), FP1→F4 (0.14, 0.19, 8.01E-15), FP1→FCz (0.16, 0.21, 1.30E-14), FP2→F7 (0.05, 0.189, 1.43E-52), FP2→F3(0.14, 0.19, 1.86E-13), FP2→Fz (0.13, 0.21, 4.72E-25), FP2→F8 (0.09, 0.18, 3.30E-19), FP2→FCz (0.15, 0.21, 4.81E-11), FP2→C3 (0.15, 0.189, 1.42E-05), FP2→Cz (0.16, 0.19, 3.37E-05), FP2→Pz (0.16, 0.19, 7.80E-06), F7→P7 (0.14, 0.19, 5.39E-17), F3→F8 (0.09, 0.19, 2.32E-43), F3→Pz (0.16, 0.21, 7.94E-17), Fz→F8 (0.07, 0.19, 6.60E-52), F4→F8 (0.07, 0.20, 3.37E-59), F8→P7(0.09, 0.18, 3.74E-34), C3→P8 (0.11, 0.18, 1.59E-32), C3→O2 (0.11, 0.19, 4.25E-47), P8→O1 (0.14, 0.18, 5.36E-12), O1→O2 (0.17, 0.19, 0.000751), Fz→FP1 (0.09, 0.20, 9.26E-49), P7→FP1 (0.15, 0.20, 5.41E-23), Fz→FP2 (0.10, 0.21, 1.48E-47), C3→FP2 (0.14, 0.22, 2.80E-31), Cz→FP2 (0.13, 0.25, 2.11E-53), C4→FP2 (0.17, 0.2, 2.24E-18), P7→FP2 (0.15, 0.19, 3.94E-11), Pz→FP2 (0.15, 0.24, 5.66E-40), O1→FP2 (0.15, 0.24, 5.66E-40), O2→FP2 (0.18, 0.2, 4.17E-15), F3→F7 (0.16, 0.23, 2.85E-21), Fz→F7 (0.06, 0.21, 5.20E-63), Cz→F7 (0.015, 0.19, 9.28E-89), C4→F7 (0.07, 0.25, 2.63E-74), P7→F7 (0.12, 0.25, 9.53E-51), P8→F7 (0.14, 0.20, 3.05E-16), O1→F7 (0.11, 0.22, 3.03E-33), P7→Fz (0.07, 0.22, 1.10E-62), FCz→F4 (0.18, 0.23, 1.64E-17), C3→F4 (0.13, 0.23, 6.90E-33), Cz→F4 (0.24, 0.31, 3.65E-15), C4→F4 (0.28, 0.38, 1.68E-26), P7→F4 (0.32, 0.39, 1.75E-12), Pz→F4 (0.16, 0.22, 2.11E-21), P8→F4 (0.24, 0.31, 1.50E-18), O1→F4 (0.20, 0.25, 1.32E-10), FCz→F8 (0.19, 0.23, 2.60E-08), O1→F8 (0.04, 0.19, 5.41E-72), O1→P7 (0.12, 0.22, 1.24E-36), O2→P7(0.08, 0.19, 3.48E-47), increase gradually from the first to the fourth day, with the fourth day being significantly greater than the first ($p< 0.01$). Note: (0.15, 0.19, 1.81E-07), where '0.15',' 0.19' represents the GCA feature value on the first day and the fourth day respectively, and '1.81E-07' represents the P value. Fig. 13(b) showed the increased connectivity visually.

3) α_1 Frequency Band: The GCA results of α_1 frequency band activity on the first and fourth days of training are shown below. GCA feature values of brain area combinations including FP1→F7 (0.05, 0.21, 4.66E-79), FP2→F7 (0.05, 0.20, 3.02E-67), FP2→F3 (0.13, 0.21, 4.35E-24), FP2→Fz (0.15, 0.22, 4.35E-19), FP2→FCz (0.16, 0.21, 3.95E-10), F7→Fz (0.17, 0.22, 3.36E-14), F7→P7 (0.16, 0.19, 1.50E-08), F3→F8 (0.13, 0.20, 4.36E-25), Fz→F8 (0.12, 0.21, 2.53E-38), Fz→C4 (0.22, 0.24, 0.00737), FCz→C4 (0.21, 0.24, 1.75E-05), C3→P7 (0.14, 0.20, 2.57E-22), Cz→Pz (0.11, 0.21, 7.54E-46), P7→FP1 (0.18, 0.21, 1.13E-11), O1→FP1 (0.17, 0.24, 3.03E-20), F3→FP2 (0.15, 0.22, 5.08E-22), Fz→FP2 (0.14, 0.23, 9.44E-34), FCz→FP2 (0.12, 0.22, 2.38E-43), C3→FP2 (0.19, 0.25, 4.32E-22), Cz→FP2 (0.17, 0.27, 4.00E-42), Pz→FP2 (0.18, 0.26, 8.91E-33), F3→F7 (0.08, 0.22, 1.50E-62), Fz→F7 (0.06, 0.22, 5.33E-84), FCz→F7 (0.01, 0.22 2.87E-123), C4→F7 (0.14, 0.27, 6.82E-47), Pz→F7 (0.12, 0.25, 1.24E-52), Fz→F3 (0.14, 0.24, 1.49E-34), C3→F4 (0.26, 0.33, 4.97E-19), Cz→F4 (0.32, 0.40, 3.72E-22), C4→F4 (0.33, 0.41, 6.82E-19), O1→F4 (0.22, 0.25, 9.14E-07), P7→FCz (0.20, 0.24, 1.58E-10), P8→Cz (0.17, 0.20, 9.49E-06), O1→P7 (0.09, 0.21, 3.69E-58), O2→P7 (0.07, 0.19, 2.75E-63) increase gradually from the first day to the fourth day, with the fourth day being significantly greater than the first ($p< 0.01$). Note: (0.05, 0.21, 4.66E-79), where '0.05',' 0.21' represents the GCA feature value on the first day and the fourth day respectively, and '4.66E-79' represents the P value. Fig. 13(c) showed the increased connectivity visually.

4) β_2 Frequency Band: The GCA results of β_2 frequency band activity on the first and fourth days of training are shown below. GCA feature values of brain area combinations including FP2→F7 (0.18, 0.19, 0.0013), FP2→F4 (0.19, 0.20, 0.00441), Fz→FCz (0.19, 0.21, 0.0162), P7→Fz (0.23, 0.25, 0.0013), P7→FCz (0.23, 0.26, 5.35E-06) increase gradually from the first day to the fourth day, with the fourth day being significantly greater than the first ($p< 0.01$). Note: (0.18, 0.19, 0.0013), where '0.18',' 0.19' represents the GCA feature value on the first day and the fourth day respectively,

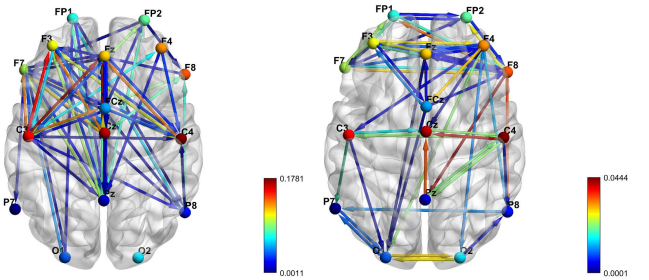

(a) (b)

Fig. 14. The changes in the pair-wise connectivity between the pre- and post-testing in the β_1 frequency band. (a) represent the channel pairs with increased connectivity, and (b) represent the channel pairs with decreased connectivity.

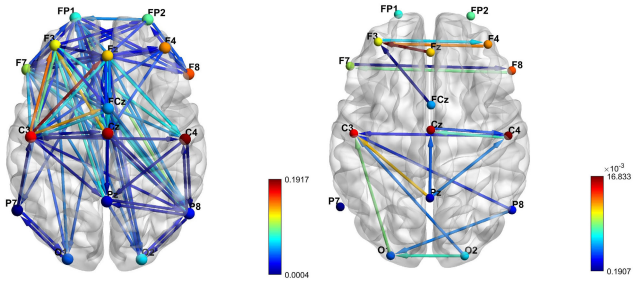

(a) (b)

Fig. 15. The changes in the pair-wise connectivity between the pre- and post-testing in the β_2 frequency band. (a) represent the channel pairs with increased connectivity, and (b) represent the channel pairs with decreased connectivity.

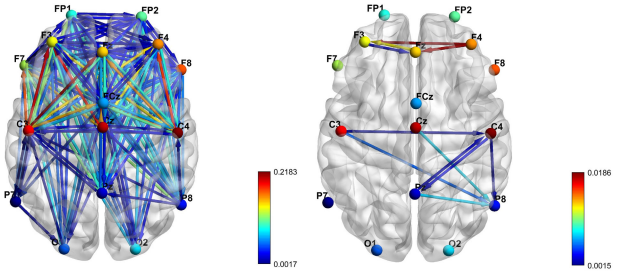

(a) (b)

Fig. 16. The changes in the pair-wise connectivity between the pre- and post-testing in the γ frequency band. (a) represent the channel pairs with increased connectivity, and (b) represent the channel pairs with decreased connectivity.

and '0.0013' represents the P value. Fig. 13(d) showed the increased connectivity visually.

5) γ Frequency Band: The GCA results of γ frequency band activity on the first and fourth days of training are shown below. GCA feature values of brain area combinations including FP1→Fz (0.16, 0.17, 4.27E-07), FP1→FCz (0.17, 0.18, 0.00182), FP2→Fz (0.16, 0.19, 5.57E-18), F4→FP2 (0.15, 0.17, 2.10E-05), F4→F7 (0.15, 0.17, 7.99E-05), FCz→F8 (0.15, 0.16, 0.0267) increase gradually from the first to the fourth day, with the fourth day being significantly greater than the feature intensity of the first day (p< 0.01). Note: (0.16, 0.17, 4.27E-07), where '0.16',' 0.17' represents the GCA feature value on the first day and the fourth day respectively, and '4.27E-07' represents the P value. Fig. 13(e) showed the increased connectivity visually.

C. The Differences in the Pairwise Connectivity of the EEG Signals Collected in the VCW Task Before and After Training

This section shows the differences in the brain connectivity between the two VCW tasks before and after the navigation training. Brain region connection diagrams are used to show the information flow between the brain regions in different frequency bands. This study focuses on the EEG channel pairs that exhibited statistical differences (p $<$ 0.01) in the β_1, β_2, and γ frequency bands between two VCW tasks.

1) β_1 Frequency Band: Fig. 14 shows the statistically significant differences ($p< 0.01$) in pair-wise connectivity (Fig. 14(a) and Fig. 14(b)) between two VCW tasks before and after training in the β_1 frequency band. The colors represent how much connectivity increased or decreased on the post-testing relative to the pre-testing.

In the β_1 frequency band, the navigation training increased mainly the connectivity within the frontal areas, between the left frontal, central, and left central areas, and between the right frontal and right central areas, while decreasing mainly the connectivity between the left/right frontal and parietal areas. β_2 frequency band

Fig. 15 shows the statistically significant differences ($p< 0.01$) in pair-wise connectivity (Fig. 15(a) and Fig. 15(b)) between two VCW tasks before and after training in the β_2 frequency band. The colors represent how much connectivity increased or decreased on the post-testing relative to the pre-testing.

In the β_2 frequency band, nearly all the connectivity increased, focusing on the left frontal areas and among the left frontal, central, and left central areas, as well as between the right temporal and the central areas, while connectivity between the left and right prefrontal or left and right frontal areas, and between the central and occipital areas decreased. γ frequency band.

Fig. 16 shows the statistically significant differences ($p< 0.01$) in pair-wise connectivity (Fig. 16(a) and Fig. 16(b)) between two VCW tasks before and after training in the γ frequency band. The colors represent how much connectivity increased or decreased on the post-testing relative to the pre-testing.

In the γ frequency band, nearly all the pairwise connectivity increased, especially between the left and right (pre)frontal areas, between the frontal, central, parietal, and occipital areas, while the connectivity between the left/right prefrontal areas and central areas, and between the right parietal and central areas decreased mainly.

IV. Discussion

A. The Necessity and Value of System Design

Only a few studies on spatial cognition have combined EEG-HMD and VR to date. VR can provide the immersive environments needed for testing spatial cognition. EEG signals and functional magnetic resonance imaging (fMRI) data can be used to quantify the active states of the brain. Bischof et al. collected EEG signals from subjects performing VR maze navigation tasks and found that θ oscillations were linked to the encoding and retrieval of spatial information [25]. Tarnanas et al. used the VR day-out task (VR-DOT) to evaluate its predictive value for patients with mild cognitive impairment

(MCI) [42], [43]. Compared to EEG, fMRI, and neuropsychological testing methods, VR-DOT could provide additional predictive information in a low-cost, computerized, and non-invasive manner. Li et al. designed a traffic road virtual simulation cognitive training system, which could strengthen subjects' cognition and memory of static control facilities such as traffic signs and markings [44]. Silvia et al. compared the differences in EEG θ oscillation between males and females in VR space navigation tasks and found that female participants had stronger θ oscillations when processing road signs as navigation aids [27]. Jaiswal et al. combined BCI with VR to observe the differences in EEG signals during the coding and retrieval phases of spatial memory tasks [26]. These experiments have demonstrated the benefit of combining BCI and VR technology for spatial cognitive research. This study developed a home-based spatial cognitive training and evaluation system based on BCI-VR. This system used a classic experimental paradigm, "Morris water maze task" in an immersive VR environment to train the subjects' spatial cognition.

B. Data Analysis for Evaluating the System

This study analyzed the subjects' behavior in the VMWM and VCW tasks. In the VMWM tasks, task execution time, path length, and distance difference represented the ability of spatial cognition. The lower the values of these three indicators, the better the subjects' spatial cognition ability [45]. The results showed that these three indicators exhibited a downward trend throughout the entire training cycle, indicating that subjects could improve their spatial cognition ability through the training system, which was consistent with Frick et al. [46]. The variance analysis and paired T-test revealed significant differences between before and after the training in the time spent by the participants in the hidden platform phase, the path length, and the distance difference between the selected position and the actual platform position. In the VCW task, the time spent on the tasks and the completion of the task are analyzed. After 20 days of training, all seven subjects took less time to complete the VCW task, and the completion rate improved significantly.

There were significant differences in the EEG connectivity between brain regions in different frequency bands during the first four days of the VMWM training and between the two VCW tests conducted before and after the training. During the first four days of the training, the GCA eigenvalue ln(F) of the combination of brain regions in the δ, θ, α_1, β_2, and γ frequency bands gradually increased and showed significant differences before and after training [47]. In the test phase, the independent sample T-test was used to compare the GCA characteristics of EEG before and after the training, the GCA characteristics of the combination of brain regions in high-frequency bands such as β_1, β_2, and γ showed significant differences. In the β_1 frequency band, the navigation training increased mainly the connectivity within the frontal areas, between the left frontal, central, and left central areas, and between the right frontal and right central areas, while decreasing the connectivity between the left/right frontal and parietal areas. In the β_2 and γ frequency bands, the connectivity increased between most of the brain areas, except for the central and right parietal showing decreased correlations.

The subjects' spatial cognitive ability improved significantly after 20 days of virtual Morris water maze training, indicating that this system is effective for spatial cognitive training and evaluation. It will be necessary to recruit more participants in the future to assess its efficacy. Future research may investigate using this system to help patients with mild cognitive impairment with spatial cognitive rehabilitation. We collected and recorded the EEG signals throughout the experiment to investigate how cognitive training and EEG correlate. The automated task execution by the participants may contribute to the GCA and behavioral results. The decoded information from the EEG signals may provide a few control commands in the future. A larger sample size will be used in the subsequent investigation, with participants divided into control and experimental groups. Regrading other spatial cognition systems [48], [49], this system's architecture can be individualized and adaptively optimized.

V. Conclusion

This research created and tested a spatial cognitive training and assessment system that combines EEG-HMD and VR technology in a small, wearable package. Seven healthy individuals participated in a 20-day spatial cognitive training to test the effectiveness of the system. The results of the behavioral and EEG data analysis, as well as statistical tests, showed that the subjects' spatial cognitive abilities have improved significantly. Furthermore, their EEG connectivity changed significantly during the training period. Therefore, the EEG-HMD-based training and evaluation system has appreciable effects on spatial cognitive ability and has the potential to be used as a home-based clinical training and evaluation system for patients with spatial cognitive impairments. In the future, we will enhance the efficacy evaluation of the training program by adding standardized assessments of cognitive ability in addition to measuring the participant's performance using the system. This would enable us to make a more direct comparison of the training program with other similar approaches.

References

[1] L. Hongyu and L. Chongde, "A sturctural research on the spatial-cognitive ability of high school students," *Psychol. Sci.*, vol. 28, no. 2, pp. 269–271, 2005.

[2] E. A. Johnson and N. Adamo-Villani, "A study of the effects of immersion on short-term spatial memory," *Proc. World Acad. Sci. Eng. Technol.*, vol. 25, no. 71, p. 582, 2010.

[3] S. Chun-Ying et al., "Effects of training modes on spatial learning and memory in rats," *J. Shanxi Med. Univ.*, vol. 42, no. 7, pp. 539–541, 2011.

[4] Y. Zhou et al., "The current research of spatial cognitive evaluation and training with brain–computer interface and virtual reality," *Frontiers Neurosci.*, vol. 13, p. 1439, Feb. 2020.

[5] D. Wen et al., "Multi-dimensional conditional mutual information with application on the EEG signal analysis for spatial cognitive ability evaluation," *Neural Netw.*, vol. 148, pp. 23–36, Apr. 2022.

[6] S. L. Allison, "Spatial navigation in preclinical Alzheimer's disease," *J. Alzheimer's Disease*, vol. 52, no. 1, pp. 77–90, 2016.

[7] J. Laczó, M. Parizkova, S. D. Moffat, M. Vyhnalek, R. Andel, and J. Hort, "P1–355: The effect of early-stage Alzheimer's disease on spatial navigation strategies: A pilot study," *Alzheimer's Dementia*, vol. 12, pp. P565–P566, Jul. 2016.

[8] K. Bormans, "Virtual memory palaces to improve quality of life in Alzheimer's disease," *Alzheimer's Dementia*, vol. 14, pp. 227–232, Jan. 2016.

[9] D. Wen et al., "Feature classification method of resting-state EEG signals from amnestic mild cognitive impairment with type 2 diabetes mellitus based on multi-view convolutional neural network," *IEEE Trans. Neural Syst. Rehabil. Eng.*, vol. 28, no. 8, pp. 1702–1709, Aug. 2020.

[10] S. Tu, H. J. Spiers, J. R. Hodges, O. Piguet, and M. Hornberger, "Egocentric versus allocentric spatial memory in behavioral variant frontotemporal dementia and Alzheimer's disease," *J. Alzheimer's Disease*, vol. 59, no. 3, pp. 883–892, Jul. 2017.

[11] R. Davis and J. Ohman, "Wayfinding in ageing and Alzheimer's disease within a virtual senior residence: Study protocol," *J. Adv. Nursing*, vol. 72, no. 7, pp. 1677–1688, Jul. 2016.

[12] E. M. Migo et al., "Investigating virtual reality navigation in amnestic mild cognitive impairment using fMRI," *Aging, Neuropsychol., Cognition*, vol. 23, no. 2, pp. 196–217, Mar. 2016.

[13] S. Serino, F. Morganti, F. Di Stefano, and G. Riva, "Detecting early egocentric and allocentric impairments deficits in Alzheimer's disease: An experimental study with virtual reality," *Frontiers Aging Neurosci.*, vol. 7, p. 88, May 2015.

[14] S. Zygouris et al., "A preliminary study on the feasibility of using a virtual reality cognitive training application for remote detection of mild cognitive impairment," *J. Alzheimer's Disease*, vol. 56, no. 2, pp. 619–627, Jan. 2017.

[15] D. Chen et al., "Hexadirectional modulation of theta power in human entorhinal cortex during spatial navigation," *Current Biol.*, vol. 28, no. 20, pp. 3310–3315.e4, Oct. 2018.

[16] M. A. Guevara et al., "EEG activity during the spatial span task in young men: Differences between short-term and working memory," *Brain Res.*, vol. 1683, pp. 86–94, Mar. 2018.

[17] Y. Han, K. Wang, J. Jia, and W. Wu, "Changes of EEG spectra and functional connectivity during an object-location memory task in Alzheimer's disease," *Frontiers Behav. Neurosci.*, vol. 11, p. 107, May 2017.

[18] V. Pergher, B. Wittevrongel, J. Tournoy, B. Schoenmakers, and M. M. Van Hulle, "N-back training and transfer effects revealed by behavioral responses and EEG," *Brain Behav.*, vol. 8, no. 11, Nov. 2018, Art. no. e01136.

[19] M. de Tommaso et al., "Testing a novel method for improving wayfinding by means of a P3b virtual reality visual paradigm in normal aging," *SpringerPlus*, vol. 5, no. 1, pp. 1–12, Dec. 2016.

[20] J. Liu, M. Abd-El-Barr, and J. H. Chi, "Long-term training with a brain-machine interface-based gait protocol induces partial neurological recovery in paraplegic patients," *Neurosurgery*, vol. 79, no. 6, pp. N13–N14, 2016.

[21] A. Lechner and R. C. O. Guger, "Feedback strategies for BCI based stroke rehabilitation: Evaluation of different approaches," in *Replace, Repair, Restore, Relieve-Bridging Clinical and Engineering Solutions in Neurorehabilitation*. Cham, Switzerland: Springer, 2014, pp. 507–512.

[22] B. Koo, H. Lee, Y. Nam, and S. Choi, "Immersive BCI with SSVEP in VR head-mounted display," in *Proc. 37th Annu. Int. Conf. IEEE Eng. Med. Biol. Soc. (EMBC)*, Aug. 2015, pp. 1103–1106.

[23] A. Vourvopoulos and S. B. I. Badia, "Motor priming in virtual reality can augment motor-imagery training efficacy in restorative brain-computer interaction: A within-subject analysis," *J. NeuroEng. Rehabil.*, vol. 13, no. 1, pp. 1–14, Dec. 2016.

[24] S. B. I. Badia, A. G. Morgade, H. Samaha, and P. F. M. J. Verschure, "Using a hybrid brain computer interface and virtual reality system to monitor and promote cortical reorganization through motor activity and motor imagery training," *IEEE Trans. Neural Syst. Rehabil. Eng.*, vol. 21, no. 2, pp. 174–181, Mar. 2013.

[25] W. F. Bischof and P. Boulanger, "Spatial navigation in virtual reality environments: An EEG analysis," *CyberPsychol. Behav.*, vol. 6, no. 5, pp. 487–495, Oct. 2003.

[26] N. Jaiswal and W. S. R. Slobounov, "Encoding of visual-spatial information in working memory requires more cerebral efforts than retrieval: Evidence from an EEG and virtual reality study," *Brain Res.*, vol. 1347, pp. 80–89, Aug. 2010.

[27] S. E. Kober and C. Neuper, "Sex differences in human EEG theta oscillations during spatial navigation in virtual reality," *Int. J. Psychophysiol.*, vol. 79, no. 3, pp. 347–355, Mar. 2011.

[28] I. Tarnanas, "On the comparison of a novel serious game and electroencephalography biomarkers for early dementia screening," *Adv. Exp. Med. Biol.*, vol. 821, p. 63, Jan. 2015.

[29] T.-S. Lee et al., "A brain-computer interface based cognitive training system for healthy elderly: A randomized control pilot study for usability and preliminary efficacy," *PLoS ONE*, vol. 8, no. 11, Nov. 2013, Art. no. e79419.

[30] T. Hiraoka, T.-W. Wang, and H. Kawakami, "Cognitive function training system using game-based design for elderly drivers," *IFAC-PapersOnLine*, vol. 49, no. 19, pp. 579–584, 2016.

[31] I. Fajnerová, A. Plechatá, V. Sahula, J. Hrdlicka, and J. Wild, "Virtual city system for cognitive training in elderly," in *Proc. Int. Conf. Virtual Rehabil. (ICVR)*, Jul. 2019, pp. 1–2.

[32] K. Braeckman, "Exploratory relationships between cognitive improvements and training induced plasticity in hippocampus and cingulum in a rat model of mild traumatic brain injury: A diffusion MRI study," *Brain Imag. Behav.*, vol. 14, pp. 2281–2294, Dec. 2020.

[33] S. Jirayucharoensak, P. Israsena, S. Pan-ngum, S. Hemrungrojn, and M. Maes, "A game-based neurofeedback training system to enhance cognitive performance in healthy elderly subjects and in patients with amnestic mild cognitive impairment," *Clin. Interventions Aging*, vol. 14, pp. 347–360, Feb. 2019.

[34] R. Morris, "Developments of a water-maze procedure for studying spatial learning in the rat," *J. Neurosci. Methods*, vol. 11, no. 1, pp. 47–60, May 1984.

[35] R. S. Astur, M. L. Ortiz, and R. J. Sutherland, "A characterization of performance by men and women in a virtual Morris water task: A large and reliable sex difference," *Behavioural Brain Res.*, vol. 93, nos. 1–2, pp. 90–185, 1998.

[36] K. Horecka. (2017). *Deep Learning for Virual Moris Water Maze (vMWM)*. [Online]. Available: https://github.com/kevroy314/MSL-VirtualMorrisWaterMaze.

[37] J. P. Yuan, *Research on Spatial Cognitive Training and Evaluation System Integrating Brain-Computer Interface and Virtual Reality*. Qinhuangdao, China: Yanshan Univ., 2019.

[38] A. Delorme and S. Makeig, "EEGLAB: An open source toolbox for analysis of single-trial EEG dynamics including independent component analysis," *J. Neurosci. Methods*, vol. 134, no. 1, pp. 9–21, Mar. 2004.

[39] A. Brzezicka, M. Kamiński, J. Kamiński, and K. Blinowska, "Information transfer during a transitive reasoning task," *Brain Topography*, vol. 24, no. 1, pp. 1–8, Mar. 2011.

[40] K. J. Blinowska and J. Zygierewicz, *Practical Biomedical Signal Analysis Using MATLAB*. Boca Raton, FL, USA: CRC Press, 2011.

[41] F. Vecchio and C. Babiloni, "Direction of information flow in Alzheimer's disease and MCI patients," *Int. J. Alzheimer's Disease*, vol. 2011, Feb. 2011, Art. no. 214580.

[42] I. Tarnanas, A. Tsolakis, and M. Tsolaki, "Assessing virtual reality environments as cognitive stimulation method for patients with MCI," in *Technologies of Inclusive Well-Being*. Berlin, Germany: Springer, 2014, pp. 39–74.

[43] I. Tarnanas, M. Tsolaki, T. Nef, R. M. Müri, and U. P. Mosimann, "Can a novel computerized cognitive screening test provide additional information for early detection of Alzheimer's disease?" *Alzheimer's Dementia*, vol. 10, no. 6, pp. 790–798, Nov. 2014.

[44] Z. Y. Li et al., "Design of virtual simulation cognitive training system for common road traffic static control facilities," *Res. Explor. Ation. Lab.*, vol. 37, no. 6, pp. 107–111, 2018.

[45] J. J. Zhou, "The methodology of Morris water maze in detecting e learning and memory level of animals," *Chin. J. Gerontol.*, vol. 37, no. 24, pp. 6274–6277, 2017

[46] K. M. Frick and J. E. Gresack, "Sex differences in the behavioral response to spatial and object novelty in adult C57BL/6 mice," *Behav. Neurosci.*, vol. 117, no. 6, pp. 1283–1291, 2003.

[47] J. Kaiser and W. Lutzenberger, "Induced gamma-band activity and human brain function," *Neuroscientist*, vol. 9, no. 6, pp. 475–484, Dec. 2003.

[48] T. Guzsvinecz, M. Szeles, E. Perge, and C. Sik-Lanyi, "Preparing spatial ability tests in a virtual reality application," in *Proc. 10th IEEE Int. Conf. Cognit. Infocommunications (CogInfoCom)*, Oct. 2019, pp. 363–368.

[49] R. Molina-Carmona, M. Pertegal-Felices, A. Jimeno-Morenilla, and H. Mora-Mora, "Virtual reality learning activities for multimedia students to enhance spatial ability," *Sustainability*, vol. 10, no. 4, p. 1074, Apr. 2018.